Utility of AVHRR Channels 3 and 4 in Land-Cover Mapping

A. G. Kerber and *J. B. Schutt*
NASA Goddard Space Flight Center, Greenbelt, MD 20771

ABSTRACT: Imagery collected on 11 July 1981 from the Advanced Very High Resolution Radiometer aboard the NOAA-7 spacecraft was used in a four-channel (channels 1 to 4) classification study for forest, agriculture/grass, and urban categories. The class signatures composing these categories were compared using the transformed divergence algorithm. Separability in all instances was found to be dominated by emitted radiation—more so by channel 3 (3.55 to 3.93 μm) than by channel 4 (10.5 to 11.3 μm). Laboratory spectra obtained for the 3.55 to 3.93-μm region showed that for leaves the transmission was virtually zero, and the reflectances on the leaves and soil investigated were about three percent. Thus, emitted radiation dominated reflected radiation as the mechanism responsible for class separability in this spectral region. The enhancement in the separability contributed by channel 3 over that of channel 4 resulted primarily from the temperature dependence of the Planck function, and to a lesser extent by the increased transmission within channel 3 relative to channel 4.

BACKGROUND

When land-cover inventory and monitoring require frequent coverage over large areas, the Advanced Very High Resolution Radiometer (AVHRR) onboard the NOAA-6, NOAA-7, and NOAA-8 satellites provides the best opportunity to meet these requirements. These satellites, operating at an altitude of approximately 820 kilometres, have a mean orbital period of 102 minutes. The AVHRR sensor has a scan angle of ±56 degrees from nadir, resulting in a swatch width of 2258 kilometres and a spatial resolution of 1.1 km at nadir. While the repeat cycle for near-nadir viewing is nine days, the large swath width provides daily coverage. Although this daily coverage results in different look angles for the same site, complicating radiometric and geometric comparisons between different dates, there are potentially more chances of obtaining useable data than with the nine-day nadir cycle.

The AVHRR has five spectral channels, four of which have been utilized in this study: 0.58 to 0.68 μm (channel 1), 0.725 to 1.10 μm (channel 2), 3.55 to 3.93 μm (channel 3), and 10.5 to 11.3 μm (channel 4) (Kidwell, 1984). Channels 1 and 2 are spectrally similar to MSS channels 5 and 7, respectively. Channel 3 is transitional in its spectral response because it sits spectrally at the tail of the solar spectrum and at the leading edge of the emitted spectrum. Channel 4 detects only emitted radiation.

Data from channels 1 and 2 of AVHRR have been used as input to various vegetation indices to provide a greenness index for a variety of vegetation applications (Norwine and Greegor, 1983; Tucker *et al.*, 1982; Gray and McCrary, 1981a, 1981b; Schneider *et al.*, 1981, 1982). Extensive work using AVHRR data for general vegetative land-cover mapping and dynamics on a regional scale has been done by Tucker *et al.*, (1982, 1985). In these studies over the continent of Africa, variation in the extent and density of green-leaf vegetation corresponded with patterns of rainfall as well as drought conditions and provided an estimate of primary productivity and land-cover classification.

On the other hand, work performed using classified AVHRR data has been more limited. The applicability of using land cover derived from classified AVHRR data for input to hydrological models was assessed by Ormsby (1982), and the Bureau of Land Management used classified AVHRR data to develop a fire fuels map in Oregon. A classification study comparing mapping accuracies over the Chesapeake Bay region, using MSS and AVHRR data obtained from both satellites on 11 July 1981, was reported by Gervin *et al.* (1983). An unsupervised approach was used to develop land-cover classification signatures (training statistics) for both AVHRR and MSS images. The land-cover classifications that resulted were then registered to land-cover maps produced by photointerpreting aerial photography onto 12 USGS 7.5-minute (1:24,000-scale) topographic maps and digitizing the results to provide a pixel-by-pixel comparison. Their findings demonstrated that, although the spatial resolution of these sensors was considerably different (1.1 km for AVHRR and 80 metres for MSS), the overall Level I land-cover mapping accuracies were relatively similar—71.9 pecent and 76.8 percent for AVHRR and MSS, respectively. Mapping accuracies for forest, agriculture/grass, and urban varied among these two sensors. While AVHRR performed considerably better than MSS in discriminating the urban category (80.8 percent to 64.9 percent), the results for the

PHOTOGRAMMETRIC ENGINEERING AND REMOTE SENSING,
Vol. 52, No. 12, December 1986, pp. 1877–1883.

0099-1112/86/5212-1877$02.25/0

forest category were lower (67.8 percent compared to the MSS accuracy of 77.8 percent). The agriculture/grass accuracies were similar for the two sensors (69.8 percent for AVHRR and 71.9 percent for MSS).

The importance of channel 3 and channel 4 in contributing to this classification accuracy for the Chesapeake Bay region was reported by Kerber (1983). The response and range of digital values of channel 3 predominanted among the four channels for forest, agriculture/grass, and urban land-cover types. This paper formulates the basis for the relative importance of the AVHRR channels 1 to 4 in contributing to the classification accuracy observed over the Chesapeake Bay region in the Gervin *et al.* (1983) study.

APPROACH

The Chesapeake Bay study site covered approximately 14,000 square miles and encompassed the primarily agricultural Coastal Plain and Piedmont provinces, the forested Appalachian Mountains, the Chesapeake Bay, and the two major cities and suburbs of Balitmore, Maryland, and Washington, D.C. (see Figure 1). From aerial photography and ground truth, it was determined that forest made up 34 percent of the study area, agriculture/grass 35 percent, and urban less than 9 percent, with water, wetland, and barren comprising the remainder. The Chesapeake Bay study site was approximately 25 degrees off nadir in this AVHRR data set acquired 11 July 1981. The temperature and relative humidity were approximately 32°C (90°F) and 40 pecent at the time of overpass. Wind speed varied over the region from 12 to 18.5 km per hour (7.5 to 11.5 mph).

The four-channel AVHRR classification signatures developed in the Gervin study were used to investigate the relative importance of the AVHRR channels. An unsupervised classification approach was employed in which statistical parameters that define training classes were determined through a clustering algorithm (ISOCLS software program, *IDIMS User's Guide* (ESL, 1976)) of a 200 by 200 pixel area. The 71 spectral classes derived by the clustering algorithm were then used in a maximum likelihood algorithm to classify the study site into land-cover type. A total of 55 spectral classes from this clustering process composing the forest, agriculture/grass, and urban categories were used in this investigation.

To better understand the importance of the various channels in the classification accuracy achieved in this data set, the spectral class signatures (18 forested, 28 agricultural/grass, and 9 urban classes) were analyzed. The mean and standard deviation and the coefficient of variation for each land-cover category were calculated to characterize the spectral range of the categories and to reduce dependency on sample size among the land-cover types. The importance of the various channels and channel combinations was computed by means of the transformed divergence algorithm, a calculation derived from the means and covariance matrices of each spectral class, resulting in a statistical distance between class pairs. Transformed divergence, $D_T(X,Y)$ is given by

$$D_T(X,Y) = 2000\,(1 - e^{-D(X,Y)/8}), \qquad (1)$$

where

$$D(X,Y) = 1/2 \sum_{i=1}^{K} \sum_{j=1}^{K} (\Gamma_{ij}{}^{X} - \Gamma_{ij}{}^{Y})(\Gamma_{ij}{}^{-Y} - \Gamma_{ij}{}^{-X}) + (\Gamma_{ij}{}^{-X} + \Gamma_{ij}{}^{-Y})\,(\mu_i{}^{X} - \mu_i{}^{Y})(\mu_j{}^{X} - \mu_j{}^{Y}), \qquad (2)$$

K = channel set size,
Γ^X = covariance matrix for class X for the given channel set,
Γ^{-X} = inverse covariance matrix for class X for the given channel set, and
μ^X = mean vector for class X for the given channel set.

This algorithm provides an effective measure of statistical separability and probability of error in discriminating between various class pairs without allowing widely separated classes to contribute disproportionately to the result (Swain and Davis, 1978). The transformed divergence provided not only a method of selecting the best channel or channel combinations for land-cover discrimination but provided insights into the informational content of the AVHRR channels. Average diveregence of all class pair combinations was used in this multi-class situation, and was calculated for all four channels separately and all combinations of channels.

To evaluate the results observed in bands 3 and 4, measurements of the transmission and reflectance for selected natural and man-made materials were conducted using an infrared spectrophotometer (range 2.5 to 50.0 μm) with a specular reflectance attachment. Measurements were made at standard amplification with the angle of incidence at near normal. Deciduous leaves, soil samples, and construction materials (concrete, asphalt) were measured. The materials were measured for reflectance and transmission over the spectral intervals 3.55 to 3.93 μm and 10.5 to 12.5 μm to simulate AVHRR channels 3 and 4.

RESULTS AND DISCUSSION OF STATISTICAL ANALYSES

The means and standard deviations for each land cover category and channel are shown in Table 1. For the urban category, the differences in the means and standard deviations are sufficient to provide separability from the forest category in channel 1 and 4 and from the agriculture/grass category in

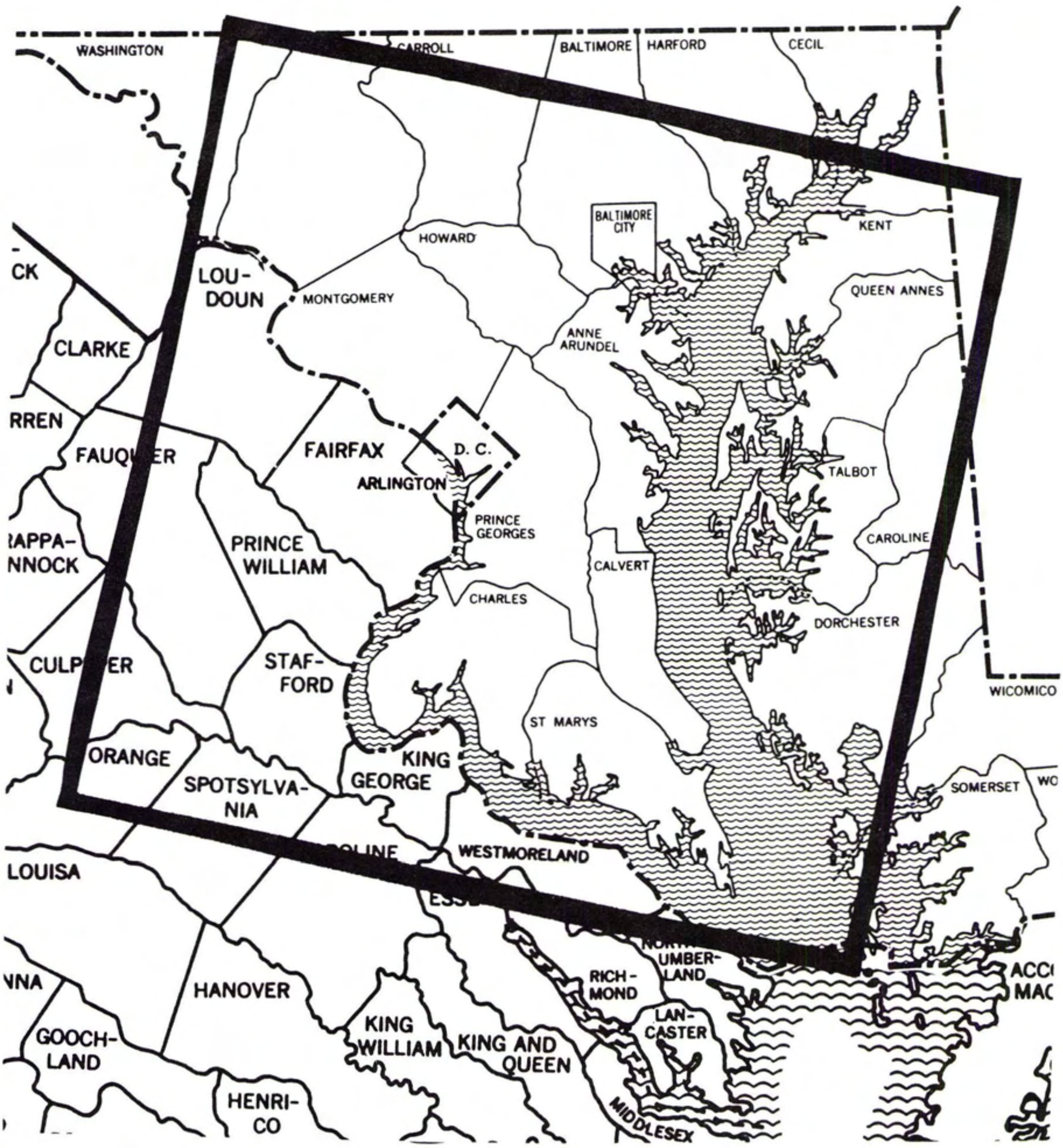

FIG. 1. Chesapeake Bay study site.

channel 2. In channel 3 there was a greater difference in means than the other channels for all categories. The mean for urban was particularly well separated from both the agriculture/grass and forest categories. The forest and agriculture categories also showed more separation in channel 3 than in channels 1, 2, and 4, but the standard deviations were larger and overlap was present. (Note than in channels 3 and 4 a smaller digital number indicates a greater brightness temperature—the reverse of most imaged data. This is a convention followed by NOAA, which registers progressively colder objects in lighter tones, e.g., clouds appear white.)

The mean and standard deviation were used to calculate the coefficient of variation, $C = s/X$, for each channel of each land-cover category to reduce dependency on sample size (Table 2). Note that the coefficients of variation were higher in channels 3 and 4 than in channels 1 and 2 for all 3 categories with the differences being less in the forest category

TABLE 1. MEAN AND STANDARD DEVIATION OF AVHRR-DERIVED SIGNATURES FOR FOREST, AGRICULTURE/GRASS, AND URBAN CATEGORIES

	Channel			
Category	1	2	3	4
Forest	86 ± 7	206 ± 12	483 ± 48	254 ± 22
Agriculture/Grass	95 ± 8	222 ± 12	418 ± 58	240 ± 29
Urban	105 ± 7	193 ± 10	252 ± 90	209 ± 24

TABLE 2. COEFFICIENT OF VARIATION OF AVHRR-DERIVED SIGNATURES FOR FOREST, AGRICULTURE/GRASS, AND URBAN CATEGORIES

	(In Percent) Channel			
Category	1	2	3	4
Forest	8.4	5.8	9.9	8.7
Agriculture/Grass	5.6	5.6	14.0	12.0
Urban	6.8	5.2	35.6	11.4

TABLE 3. AVERAGE TRANSFORMED DIVERGENCE OF COMBINED FOREST, AGRICULTURE/GRASS, URBAN CATEGORIES

Channels 1, 2, 3, 4 = 1945		
Single Set	Sets of 2	Sets of 3
3 = 1739	3, 4 = 1902	2, 3, 4 = 1938
4 = 1228	2, 3 = 1817	1, 3, 4 = 1913
1 = 908	1, 3 = 1789	1, 2, 3 = 1857
2 = 665	1, 4 = 1597	1, 2, 4 = 1744
	2, 4 = 1498	
	1, 2 = 1284	

than agriculture/grass and urban. The greatest variation was in the urban category in channel 3, reflecting the range of thermal fluxes present and implying that temperature differences between and among categories dominate reflectance differences for class separation.

To provide a basis for judging class separability, the transformed divergence was calculated from the means and covariance matrices of all class-pair combinations. For the signature set as a whole (all categories together), the divergences were averaged for all four channels, for channels individually, and for all combinations of 2 and 3 channels (Table 3). The range of divergence values provided by the transformation was from 0 to 2000. The closer the divergence approached 2000, the greater the separability. A divergence of 1700 was selected as the threshold value; lower values show a decreasing ability to discriminate among the classes (ESL Incorporated, 1979).

The single set series in Table 3 resulted in channel 3 providing the most separation among the classes with a divergence of 1739. For the single set data it was evident that the thermal contribution creates divergences substantially greater than those from the reflective channels. The combination of two channels providing the most separation were channels 3 and 4—the divergence value of 1902 approaches the 1945 value for all four channels together. For the sets of three channels, the combination 2, 3, and 4 provided a divergence of 1938 which was nearly identical to the average divergence for all four channels together. The presence of channel 3 was necessary, either singly or in sets of 2 or 3 channels, to provide a minimum separability level of 1700 or above. (The exception was the combination of channels 1, 2, and 4).

Common to all results was the increase in classification accuracy provided by the thermal channel (channel 4) and the mixed response channel (channel 3). A comparison of contrasts (differences) between means for each category (Table 1) showed that channel 4 performed better than channels 1 or 2, and channel 3 excelled relative to the other three. The coefficients of variation (Table 2) showed the same trend as the mean values for the derived signatures. For the intercategory divergence test (Table 3) the trend was the same. Divergences for single, double, and triple channel combinations were invariably increased by inclusion of the thermal channel and substantially increased over those for the reflective channels by inclusion of the mixed response channel. Clearly, channels 3 and 4 can contribute significant information for discrimination of land cover and that the emitted component of these channels is the primary basis for this discrimination.

Most recently, the dominance of channel 3 over channels 1 and 2 (imaged as the normalized vegetation index) for discriminating disturbed and virgin forest in Rondonia, Brazil was reported by Tucker *et al.* (1984). This effect was further explained by Schutt *et al.* (1985), where it was shown that the reflected component in channel 3 did not deter from its ability to distinguish these cover types using emitted radiation.

RESPONSE ANALYSES OF CHANNELS 3 AND 4

ATMOSPHERIC EFFECTS

Holben and Fraser (1984) studied the effects of atmosphere on AVHRR sensor response in Channels 1 and 2, but did not consider channels 3, 4, and 5. Conditions affecting atmospheric transmission were investigated here to determine the possible influence of atmospheric water on the responses found in channels 3 and 4.

The attenuation of electromagnetic radiation passing through the atmosphere is wavelength dependent. Spectral regions having relatively little attenuation exist. Channels 3 and 4, and 5 have been placed to take advantage of these atmospheric windows. The relative intensity of the emitted radiation in channels 3 and 4 is affected primarily by precipitable water and to a significantly lesser extent by ozone and oxygen (Bird, 1984). For the purpose of comparing the relative effect of precipitable water on channels 3 and 4, we note that to reduce the transmission below 90 percent requires about 10 cm for channel 3 and 0.9 cm for channel 4 (Hudson, 1969). Decreases in precipitable water improves atmospheric transmission; in fact, with limited amounts of precipitable water there are similar effects on atmospheric transmission within these channels. The precipitable water measurement for the study area was obtained from an isopleth map provided by the National Climatic Data Center. Precipitable water on 11 July 1981 measured 1.9 cm and was collected by vertically integrating along a path length from the surface to 500 millibars of pressure (approximately 18 to 19,000 feet) for a site outside Washington, D.C. (personal communication, National Weather Service, 1984). This amount of precipitable water provided transmission values of about 95 percent and 80 percent for channels 3 and 4, respectively (Hudson, 1969). Given this transmission difference of about 15 percent, a portion of the response difference between these channels is attributable to differential water vapor absorption.

Holben and Tucker (1985) have observed high reflectance in the 3.53 to 3.93 channel associated with clouds in South America and elsewhere. In this Chesapeake Bay data set, clouds, which appear from the satellite data to be cumulus, were present in the southern portion of the study area. However, the clouds (and shadows) were classified as distinct classes of the data, thus eliminating them from further spectral consideration.

Laboratory Spectral Measurements

Laboratory measurements using an infrared spectrophotometer with a near normal specular reflectance attachment showed near zero transmission for leaves and a reflected component of about 3 percent or less for the 3.55 to 3.93 μm region. For a loamy soil the reflectance was found to be about 3 percent with concrete and asphalt, giving similar values. Past studies have indicated little reflectivity of leaves beyond about 3 μm. Gates and Tantraporn (1952) found less than 10 percent reflectance for vegetation for an angle of incidence of 65 degrees and less than 5 percent for an angle of 20 degrees. These low reflectance values point to the dominance of the thermal component in generating signature differences, because the emittance is one minus the reflectance. Based upon these results, it has been tentatively concluded that the reflected component in channel 3 made a small contribution to the overall signature.

Explanation of Thermal Behavior

These results have demonstrated that the availability of a thermal signature and/or the ability to attribute a temperature to a category provided improved classification accuracy over purely reflective signatures. The ability of channel 3 to provide enhanced classification accuracy for daytime sensing resides in the existence of greater temperature contrasts during daylight hours (Matson and Dozier, 1981). For example, calculations show that the average flux spanning the bandwidth of channel 3 increased about nine fold between 273°K and 323°K (90° F, the air temperature of the study area), while that for channel 4 increased about two fold. The observed differences in thermal response found for these channels can be explained using Plank's Law (Mayer and Mayer, 1940) for emitted radiation (also referred to as the black body equation), i.e.,

$$F = \epsilon\, C_1/\lambda^5 \frac{1}{\exp\,(C_2/\lambda T - 1)} \frac{\text{watts}}{\text{m}^2\ \mu\text{m}} \tag{3}$$

where

$$C_1 = 3.7413 \times 10^8 \frac{\text{watts}}{\text{m}^2}(\mu\text{m}^4),$$

$$C_2 = 14388\ \mu\text{m}\ °\text{K, and}$$

ϵ is a scale factor (emissivity) representing the efficiency of the emitter.

This is a theoretical result showing the wavelength (λ) distribution of thermalized radiation as a function of body temperature (T). Application of this law to the behavior of channel 3 shows that thermalized solar radiation in this spectral region is dominated by the exponential function, i.e., $\exp(C_2/\lambda T) >> 1$, which is responsible for the rapidly rising leading edge and broadening of the black body curve with increasing temperature. To ascertain the temperature range over which channel 4 monitors peak thermal fluxes, the equation for calculating the wavelength (λ_m) where the thermal flux is maximum for any temperature was inverted, *viz*:

$$T = \frac{2897.7}{\lambda_m}\ °\text{K}. \tag{4}$$

Applying Equation 4 to channel 4 (10.5 to 11.3 μm), it is easily observed that, if the maximum thermal flux occurs at 10.5 μm, the apparent temperature is 3°C whereas, if it occurs at 11.3 μm, the apparent temperature is −16.6°C. Therefore, for temperatures greater than 3°C, emissions sensed by channel 4 are on the downside of the black body curve, where the response is approaching linearity. These divergent behaviors are responsible for the increased selectivity of channel 3 over channel 4 as the temperature is increased.

To demonstrate this effect, the differences of channel-averaged fluxes were calculated in increments of 5°C and normalized to the initial difference, viz:

$$R = \left[\frac{< F(T_i) > - < F(T_j) >}{< F(278) > - < F(273) >}\right]_{\Delta\lambda},$$

where $T_i = T_j + 5°\text{C}$, and $273 \leq T_j \leq 318$, was plotted (Figure 2) for channels 3 and 4. The notation $< >$ in combination with the subscript $\boldsymbol{\Delta\lambda}$ symbolizes the average thermal flux within the channel. The increased contrast between scenes or objects of differing thermal properties becomes readily apparent

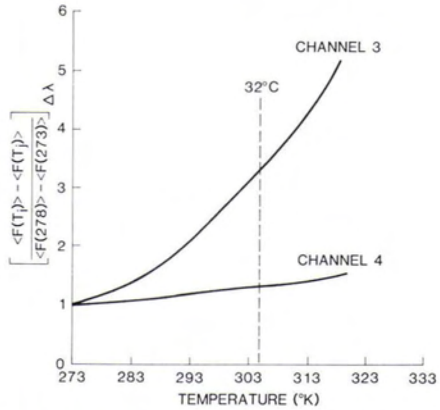

FIG. 2. Normalized flux differences plotted at 5°C intervals for channels 3 and 4.

when presented in this manner. This increased sensitivity to temperature in channel 3 provided greater contrast between categories (objects) having different optical and thermal properties. Thus, small changes in the ordinate (Figure 2) indicate larger temperature differences for channel 3 than for channel 4. This behavior demonstrates the greater sensitivity of channel 3 over channel 4 to temperature differences. Although transmission plays a role in this sensitivity, the predominant influence is determined by the Planck function. It is important to note that the wind speed, 7.5 to 11.5 mph for the study area at an ambient temperature of 90°F (32°C), apparently had little effect on the thermal contrasts between categories.

SUMMARY

The success in separating categories comprising forest, agriculture/grass, and urban was found to be related to temperature differences between categories because in all instances channels 3 and 4 increased the transformed divergence. The increase in all divergences provided by channel 3 resulted primarily from the exponential behavior of the Planck function in the 3.55- to 3.93-μm region and by the higher transmissivity within channel 3 relative to channel 4. Preliminary investigations from our long-term field studies on the effect of season, time of day, air temperature, and wind speed indicate that these factors can affect the separability of land-cover features using thermal information within channels 3 and 4.

REFERENCES

Bird, R. E., 1984. A Simple, Solar Spectral Model for Direct-Normal and Diffuse Horizontal Irradiance, *Solar Energy*, Vol. 32, No. 4, pp. 461–471.

ESL (Electromagnetic Systems Laboratory, Inc.), 1979. *IDIMS User's Guide*. Technical Memorandum ESL-TM705, Sunnyvale, California.

Gates, D. M., and W. Tantraporn, 1952. The Reflectivity of Deciduous Trees and Herbaceous Plants in the Infrared to 25 Microns, *Science*, Vol. 115, pp. 613–616.

Gervin, J. C., A. G. Keber, R. G. Witt, Y. C. Lu, and R. Sekhon, 1983. Comparison of Level I Land Cover Classification Accuracy for MSS and AVHRR Data, *Seventeenth International Symposium on Remote Sensing of Enviornment*, Ann Arbor, Michigan, 9–13 May.

Gray, J. I., and D. G. McCrary, 1981a. *Meterological Satellite Data: A Tool to Describe the Health of the World's Agriculture*, AgRISTARS Report EW-N1-04042. Johnson Space Center, Houston, Texas.

———, 1981b. The Environmental Vegetative Index—A Tool Potentially Useful for Arid Lane Management, *Fifteenth Conference on Agriculture and Forest Meteorology and Fifth Conference on Biometeorology*, Anaheim, California, 1–3 April.

Holben, B. N., and R. S. Fraser, 1984. Effects of Atmosphere and View and Illumination Geometry on Visible and Near IR AVHRR Radiance Data, *International Journal of Remote Sensing*, 5, 145.

Hudson, R. D., Jr., 1969. *Infrared System Engineering*. John Wiley & Sons, New York.

Kidwell, K. B., 1984. *NOAA Polar Orbirer Data User's Guide*. National Oceanic and Atmospheric Administration, Satellite Data Services Division, Washington, D.C.

Kerber, A. G., 1983. Utility of the Advanced Very High Resolution Radiometer (AVHRR) Middle Infrared and Thermal Channels in Land Cover Mapping, *National Conference on Resource Management Applications: Energy and Environment*, Vol. VII, pp. 32–40.

Matson, M., and J. Dozier, 1981. Identification of Subresolution High Temperature Sources Using a Thermal IR Sensor, *Photogrammetric Engineering and Remote Sensing*, Vol. 47, No. 9, pp. 1311–1318.

Mayer, J. E., and M. G. Mayer, 1940. *Statistical Mechanics*, John Wiley and Sons, New York, pp. 365–374.

National Weather Service, 1981. *Isopleth Maps of United States*, National Climate Data Center, Ashville, North Carolina.

Norwine, J. and D. H. Greegor, 1983. Vegetation classification based on AVHRR satellite imagery, *Remote Sensing of Environment*, Vol. 13, pp. 69–87.

Ormsby, J. P., 1982. Classification of Simulated and Actual NOAA-6 AVHRR Data for Hydrologic Land Surface Feature Definition, *IEEE Transactions on Geoscience and Remote Sensing*, Vol. TE-20, July, No. 3, pp. 262–268, July 1982.

Schneider, S. R., D. F. McGinnis, Jr., and J. A. Gatlin, 1981. *Use of NOAA/AVHRR Visible and Near-Infrared Data for Land Remote Sensing*, NOAA Technical Report No. 5584, Department of Commerce, Washington, D.C.

Schneider, S. R., and D. R. McGinnis, Jr., 1982. The NOAA/AVHRR: A New Satellite Sensor for Monitoring Crop Growth, *Machine Processing of Remotely Sensed Data Symposium*, Purdue/LARS, West Lafayette, Indiana, pp. 281–289.

Schutt, J. B., B. N. Holben, and A. G. Kerber, 1985. *Separating Emitted and Reflected Components in AVHRR Channel 3 for Vegetation-Soil Discrimination*, NASA Goddard Space Flight Center, Greenbelt, Maryland, unpubished results.

Swain, P. H., and S. M. Davis, 1978. *Remote Sensing: The Quantitative Approach*. McGraw-Hill, Inc., New York, pp. 164–174.

Tucker, C. J., J. A. Gatlin, S. R. Schneider, and M. A. Ruchinos, 1982. Monitoring Vegetation in the Nile Delta with NOAA-6 and NOAA-7 AVHRR Imagery. *Proceedings of the International Symposium on Remote Sensing of Environment*, Cairo, Egypt, 19–25 January, pp. 973–987.

Tucker, C. J., B. N. Holben, and T. E. Goff, 1984. Intensive forest clearing in Rondonia, Brazil as detected by satellite remote sensing. *Remote Sensing of Environment* 15, pp. 255–261.

Tucker, C. J., J. R. G. Townshend, and T. E. Goff, 1985. African Land-Cover Classification Using Satellite Data. *Science*, Vol. 227, No. 4685, pp. 369–375.

(Received 3 August 1985; accepted 7 October 1985; revised 8 May 1986)

XIIth National Surveying Teacher's Conference "Surveying the Future"

University of Wisconsin, Madison, Wisconsin 6–10 July 1987

This Conference on Education in Cartography, Geodesy, Geographic Information Systems, Photogrammetry, Remote Sensing, and Surveying — hosted by the University of Wisconsin in cooperation with the American Congress on Surveying and Mapping, the American Society for Photogrammetry and Remote Sensing, the Institute for Land Information, and the Wisconsin Society of Land Surveyors — will feature educational papers in the following technical areas:

- Surveying
- Remote Sensing
- Photogrammetry
- Geodesy
- Geographic Information Systems/Land Information Systems
- Multipurpose Cadastres
- Cartography

Specific topic areas include

- Changing Education Requirements
- Curriculum Development
- Emerging Technologies
- Computers in Education
- Accreditation
- Continuing Education
- Job Market/Job Placement
- Equipment
- Program Administration
- Research Needs
- Textbooks and other Resource Materials
- Programs for 2 Year/4 Year/Graduate Level
- History of Surveying Education
- Student Professional Organizations

Plan to attend. For additional information, please contact

Prof. Paul R. Wolf, Coordinator
XXIth National Surveying Teacher's Conference
Department of Civil and Environmental Engineering
Room 1204 Engineering Building
University of Wisconsin
Madison, WI 53706
Tele. (608) 262-1978